Stem Cell Reports, Volume *8*

Supplemental Information

Directed Differentiation of Human Pluripotent Stem Cells to Microglia

Panagiotis Douvaras, Bruce Sun, Minghui Wang, Ilya Kruglikov, Gregory Lallos, Matthew Zimmer, Cecile Terrenoire, Bin Zhang, Sam Gandy, Eric Schadt, Donald O. Freytes, Scott Noggle, and Valentina Fossati

Supplemental Information

Supplemental Data

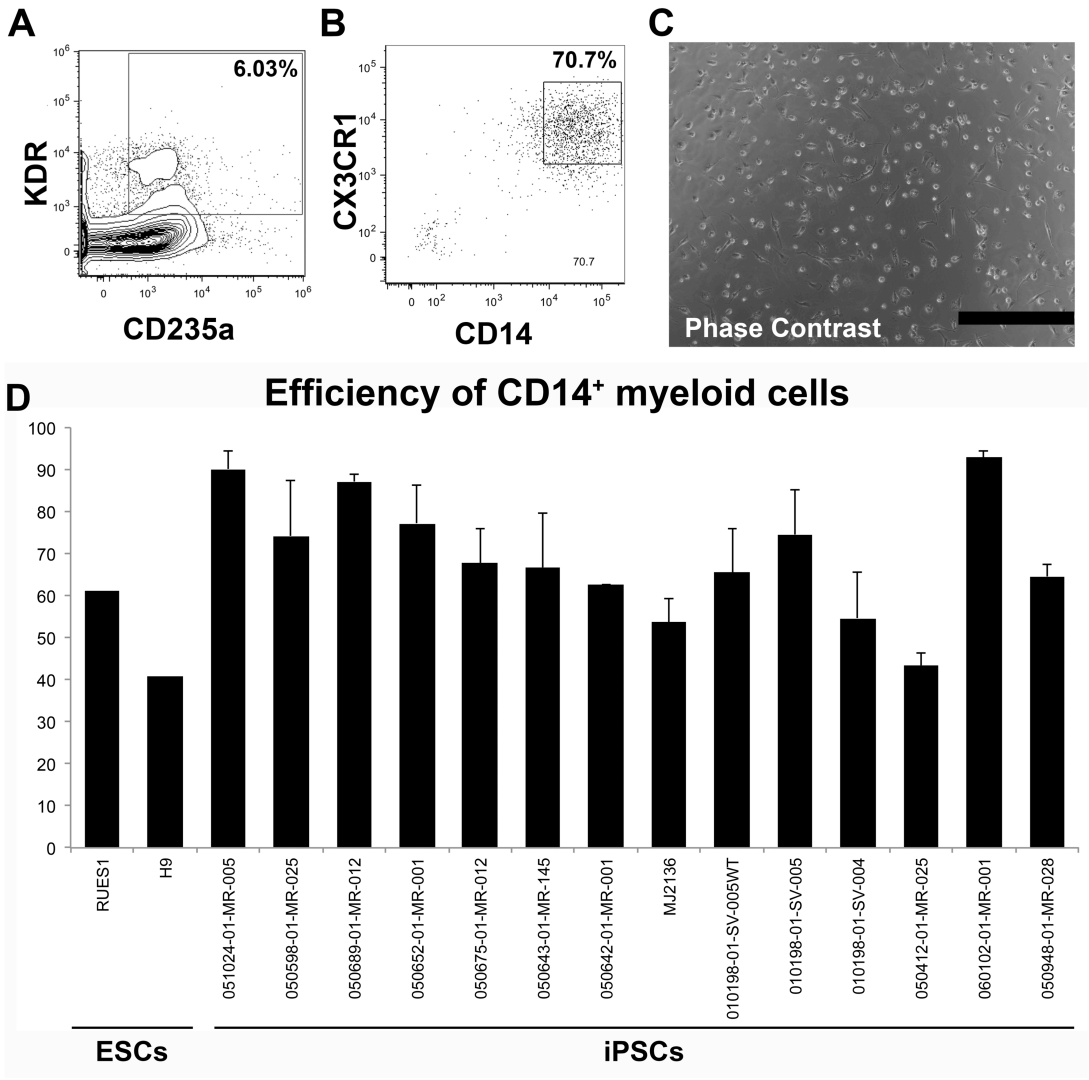

Figure S1. Microglial progenitors. Related to Figure 1. (A) Primitive hemagioblasts could be identified as $KDR^{+}CD235a^{+}$ in the adherent fraction of day 6 cultures. **(B)** Representative plot of the sorting gate used to isolate $CD14^{+}CX3CR1^{+}$ microglial progenitors via FACS between day 25 and 50 of differentiation. **(C)** Phase contrast image of plated microglial progenitors two days after isolation. Scale bar is 500µm. **(D)** Graph showing the performance of 2 ESC and 14 iPSC lines in generating $CD14^{+}$ myeloid progenitors, quantified by flow cytometry. For the iPSC lines, data were pooled from 2-7 different isolations from 1-3 independent differentiation experiments. ESCs lines are shown for comparison.

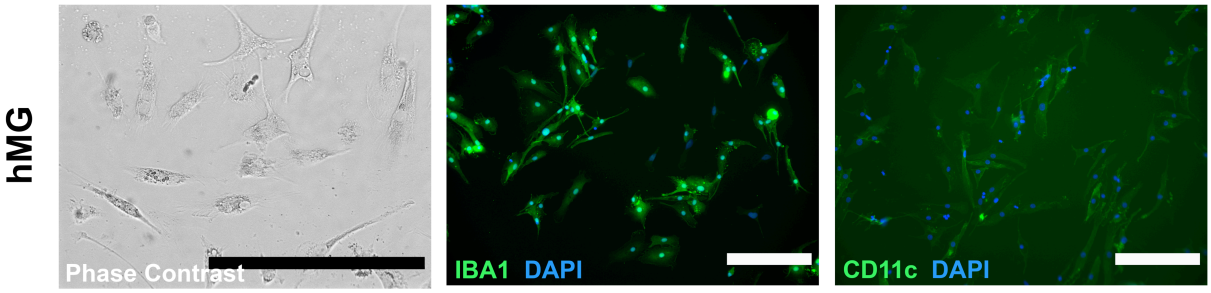

Figure S2. Characterization of human primary microglia (hMG). Related to Figure 2. Panel of representative images of hMG in phase contrast, and after immunofluorescent labeling for IBA1 and CD11c. Scale bars from left to right are 500µm, 200µm and 200µm

		iPSC-MG	hMG-SF	hhM	PB-M(-)	iPSC-MG/ hMG-SF	iPSC-MG/ hhM	iPSC-MG/ PB-M(-)
Common in all 3 studies	TREM2	10.0	8.7	4.5	8.6	1.2	2.2	1.2
	SLCO2B1	9.7	9.7	7.1	6.4	1.0	1.4	1.5
	HEXB	9.6	9.1	8.5	9.3	1.0	1.1	1.0
	GPR34	8.8	7.6	3.4	4.3	1.2	2.5	2.0
	OLFML3	3.4	5.7	6.9	1.6	0.6	0.5	2.2
	SLC2A5	2.9	4.3	3.8	6.9	0.7	0.8	0.4
	P2RY12	2.4	1.2	-3.6	-2.9	2.0	-0.7	-0.8
	P2RY13	1.1	3.0	-1.6	-1.1	0.4	-0.7	-1.0
	TMEM119	-0.5	2.7	4.7	-2.5	-0.2	-0.1	0.2
	LIPH	-4.4	-3.4	-1.7	-2.2	1.3	2.6	2.0
Butovsky & Bennett	CTSD	11.0	12.5	9.3	11.7	0.9	1.2	0.9
	TGFBR1	9.2	7.4	9.7	7.6	1.2	1.0	1.2
	ENTPD1	8.3	6.3	5.1	6.0	1.3	1.6	1.4
	IL10RA	8.2	7.0	7.6	8.5	1.2	1.1	1.0
	LAIR1	7.2	8.4	7.2	8.0	0.9	1.0	0.9
	CYSLTR1	5.6	1.4	0.7	1.7	3.8	7.6	3.3
	BLNK	4.8	4.8	0.5	2.5	1.0	9.7	2.0
	RAB3IL1	4.8	4.7	2.8	3.0	1.0	1.7	1.6
	GOLM1	4.5	3.8	6.8	3.5	1.2	0.7	1.3
	PMEPA1	4.1	3.6	4.2	2.2	1.1	1.0	1.9
	OPHN1	3.6	3.4	2.6	3.5	1.0	1.4	1.0
	CCR5	3.6	6.1	4.7	5.5	0.6	0.8	0.6
Butovsky & Hickman	F11R	8.0	7.6	6.4	8.6	1.1	1.3	0.9
	ADORA3	7.0	7.4	1.4	1.7	0.9	4.9	4.1
	SPINT1	6.9	5.2	3.0	7.8	1.3	2.3	0.9
	CCL4	5.0	6.5	8.0	1.7	0.8	0.6	2.9
	CRYBB1	3.2	3.2	1.0	-1.1	1.0	3.2	-2.9
	CX3CR1	0.8	-5.7	-1.2	-3.1	-0.1	-0.6	-0.2
	ANG	0.4	0.6	0.6	1.5	0.7	0.8	0.3
Hickman & Bennett	LAG3	-2.4	0.2	-2.0	-1.6	-11.1	1.2	1.4
	GAL3ST4	3.0	4.3	2.7	-0.8	0.7	1.1	-3.9

Table S1. Expression of murine microglial signature genes in human cells. Related to Figure 3. Normalized mean expression (log_2 transformed CPM) for 31 genes that have been identified as microglial signature genes by at least two out of three independent murine studies (Hickman et al., 2013, Butovsky et al., 2014 and Bennett et al., 2016). Genes in red are consistently higher in microglia than macrophages.

	iPSC-MG1	iPSC-MG2	iPSC-MG3	iPSC-MG4	iPSC-MG5	iPSC-MG6	hMG-SF	hMG
C1QA	9.2	8.5	9.1	9.5	7.9	7.9	8.6	10.2
GAS6	7.0	6.0	7.6	7.0	6.7	6.2	5.4	5.0
GPR34	9.2	8.5	9.1	8.9	8.2	8.0	7.6	8.5
MERTK	7.6	7.3	7.7	8.5	8.8	8.6	8.6	8.3
P2RY12	4.2	0.4	3.0	3.2	0.9	1.6	1.2	5.7
PROS1	6.2	6.4	6.8	6.8	6.0	5.7	4.7	4.5

Table S2. Expression of the six human microglial validated signature genes in the microglial samples. Related to Figure 3. Expression of the selected genes in every microglial sample from the RNAseq data. Values are $\log_2$ transformed CPM.

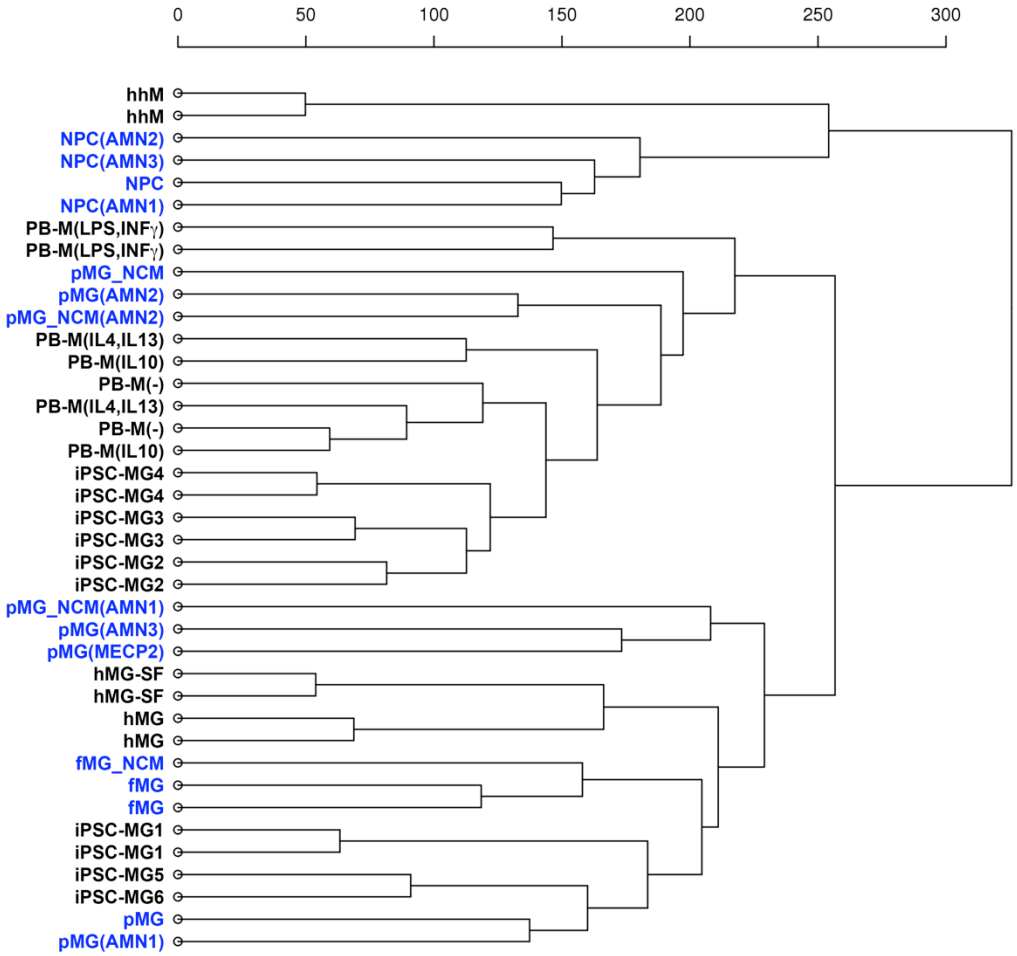

Figure S3. Comparison of RNA sequencing data to Muffat et al., 2016. Related to Figure 3. Dendrogram showing hierarchical clustering of our RNA sequencing data with data obtained from an independent study (Muffat et al., 2016) on iPSC-derived microglia (marked in blue). Analysis is based on global RNA expression after batch correction.

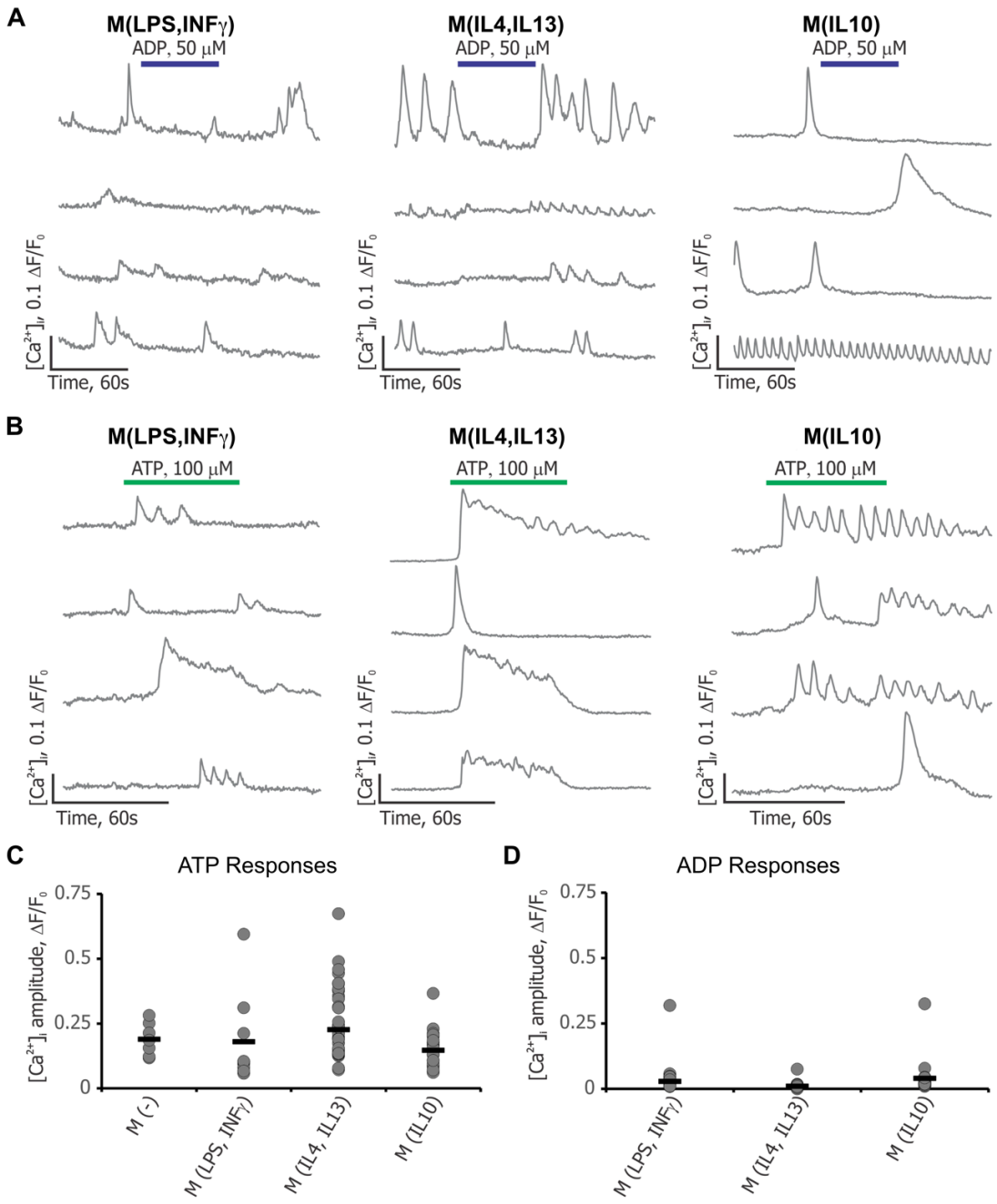

Figure S4. Intracellular Ca^{2+} transients in human peripheral blood macrophages. Related to Figure 4. Four example traces of intracellular Ca^{2+} changes during **(A)** ADP or **(B)** ATP application in macrophages polarized with (LPS,INFγ), (IL4,IL13) and (IL10). Bars represent duration of ADP (in A) or ATP (in B) application. Statistical analysis for the amplitudes of $[Ca^{2+}]_i$ transients of **(C)** ATP-responsive or **(D)** ADP-responsive macrophages. Maximum amplitude of $[Ca^{2+}]_i$ transient for each responsive cell is presented as a grey dot. The number of responsive cells is as follows: M(-) 7; M(LPS,INFγ) 9; M(IL4,IL13) 53; M(IL10) 23. Blood samples from 1-3 individuals were used to isolate monocytes that were differentiated to different macrophage subtypes.

Cell Lines	Health Status	Sex	Age	Reprogr. Method	Progenitor Efficiency	MG Markers	RNAseq	Cytokine Profiler	Phagocytosis	ADP Response	Movie
hESC RUES1	unk.	M	N/A	N/A	X$	X					
hESC H9	unk.	F	N/A	N/A	X$						
iPSC 051024-01-MR-005	w.t.	M	29	Aut. mRNA	X$	X#	X#$			X	X
iPSC 050598-01-MR-025	w.t.	M	53	Aut. mRNA	X$	X#	X#$			X	X
iPSC 050689-01-MR-012	w.t.	M	27	Aut. mRNA	X$	X#	X#$				
iPSC 050652-01-MR-001	w.t.	F	45	Aut. mRNA	X$	X		X#		X#	X
iPSC 050675-01-MR-012	w.t.	M	34	Aut. mRNA	X$		X#$				
iPSC 050643-01-MR-145	w.t.	M	25	Aut. mRNA	X$	X#	X#$	X#	X#		
iPSC 050642-01-MR-001	w.t.	M	69	Aut. mRNA	X$	X#	X#$				
iPSC MJ2136	w.t.	M	unk.	Sendai	X$	X			X		
iPSC 010198-01-SV-005WT	w.t.	M	68	Sendai*	X$						
iPSC 010198-01-SV-005	PD	M	68	Sendai	X$						
iPSC 010198-01-SV-004	PD	M	68	Sendai	X$	X					
iPSC 050412-01-MR-025	PD	M	63	Aut. mRNA	X$						
iPSC 060102-01-MR-001	MS	M	56	Man. mRNA	X$	X#				X	X
iPSC 050948-01-MR-028	AD	F	40	Aut. mRNA	X$				X	X	X$
hMG	unk.	unk.	fetal	N/A	N/A	X$	X#$	X#	X#	X#	X
hMG-SF	unk.	unk.	fetal	N/A	N/A	X	X#$	X#	X#	X#	X
PB-M(-)	unk.	unk	adult	N/A	N/A	X	X#$	X#	X#	X#	X
PB-M(INFγ,LPS)	unk.	unk.	adult	N/A	N/A	X	X#$	X#	X	X$	X
PB-M(IL4,IL13)	unk.	unk.	adult	N/A	N/A	X	X#$	X#	X	X$	X
PB-M(IL-10)	unk.	unk.	adult	N/A	N/A	X	X#$	X#	X	X$	X

Table S3. Demographic information and specific assay performed for every line described in this manuscript. Related to Experimental Procedures. Table summarizing demographic information, reprogramming method and specific assays performed with each line. "MG Markers" column includes data from flow cytometry and immunofluorescence. MG: Microglial, unk.: unknown, N/A: not applicable, Aut. mRNA: Automated mRNA/miRNA method, Man. mRNA: Manual mRNA/miRNA method. *CRISPR/Cas9 corrected PD line, #Data shown in a main figures, $Data shown in supplemental items.

Supplemental Experimental Procedures

All incubations were performed in a 37°C incubator with 5% CO_2 and all growth factors are human recombinant proteins purchased from R&D Systems, unless otherwise stated. All media contain 1X Penicillin/Streptomycin (P/S) or 1X Antibiotic-Antimycotic (Life Technologies). RT: room temperature.

Detailed information on pluripotent stem cell lines and culture conditions

RUES1 and H9 are NIH approved human ESC lines. All iPSC lines were derived from skin biopsies of de-identified donors upon specific institutional review board approvals and informed consent. The control iPSC lines 050643-01-MR-145 (25 y.o. male), 050652-01-MR-001 (45 y.o. female), 050598-01-MR-025 (53 y.o. male), 051024-01-MR-005 (29 y.o. male), 050689-01-MR-012 (27 y.o. male), 050675-01-MR-012 (34 y.o. male), 050642-01-MR-001 (69 y.o. male), the PD line 050412-01-MR-025 (63 y.o. male) and the AD line 050948-01-MR-028 (40 y.o. female) were reprogrammed using the NYSCF global stem cell array with the mRNA/miRNA method (StemGent) (Paull et al., 2015). 060102-01-MR-001 (56 y.o. male) was reprogrammed manually from a primary progressive multiple sclerosis patient, using mRNA/miRNA (Douvaras et al., 2014). 010198-01-SV-004 and 010198-01-SV-005 are two distinct clones reprogrammed with Sendai virus from a PD patient (68 y.o. male) with a GBA N370S mutation (Woodard et al., 2014) whereas 010198-01-SV-005WT is a CRISPR/Cas9 corrected line (unpublished; kind gift from Dr. Aiqun Li). MJ2136 was a kind gift from Dr. Ricardo Feldman and was reprogrammed with Sendai virus from a healthy control (Panicker et al., 2014).

The human primary microglia and hepatic macrophages were purchased from ScienCell along with Microglia Medium and Macrophage Medium (ScienCell).

PSC lines were cultured and expanded onto Matrigel-coated dishes in mTeSR1 medium (StemCell Technologies). Lines were passaged every 3-4 days using enzymatic detachment with Stempro Accutase (Life Technologies) for 5 min and re-plated in mTeSR1 medium with 10μM Rock Inhibitor (Y2732, Stemgent) for 24 hours.

Isolation of myeloid progenitors

Cells from the supernatant fraction of the cultures were incubated with CX3CR1 and/or CD14 conjugated primary antibodies (see antibody table) or their respective isotype controls for 40 min on ice. Cells were then washed in FACS buffer (PBS, 0.5% BSA, 2mM EDTA, 20mM Glucose), pelleted at 300g for 6 min and resuspended in FACS buffer containing DAPI for dead cell exclusion. $CD14^+$ or $CD14^+CX3CR1^+$ cells were isolated via FACS on an ARIA-IIu™ Cell Sorter (BD Biosciences) using the 100μm ceramic nozzle, and 20 psi.

Freezing and thawing of the myeloid progenitors

Myeloid progenitor cells were frozen after isolation in cryogenic vials (Thermo Scientific) in freezing medium consisting of 90% FBS (Life Technologies) and 10% DMSO (Sigma-Aldrich). Cells were then transferred into a Mr.Frosty (Thermo Scientific) container and placed overnight at -80°C. The next day, cryogenic vials were transferred to liquid nitrogen for long-term storage.

To thaw the cells, the cryogenic vial was transferred in a 37°C water bath for 1-2 min, until partially thawed. Under a laminar flow hood, RPMI-1640 medium was added to 5X the original volume of the vial. Cell were then centrifuged at 300g for 6 min, resuspended in the appropriate amount of medium and plated onto tissue culture treated plastic.

Detailed microglial differentiation protocol

PSCs were plated onto Matrigel (BD Biosciences) in a $15x10^3$ cells/cm^2 density in mTeSR1 medium containing 10μM Rock Inhibitor for 24 hours. When individual colonies were visible (usually 2-4 days after plating), differentiation was induced by providing mTeSR Custom medium (StemCell Technologies), containing 80ng/ml BMP4. mTeSR Custom medium is mTeSR1 medium without Lithium Chloride, GABA, Pipecolic Acid, bFGF and TGFβ1 (Stem Cell Technologies). The medium was changed daily for 4 days, when cells were induced with StemPro-34 SFM (containing 2mM GutaMAX-I, Life Technologies) supplemented with 25ng/ml bFGF, 100ng/ml SCF and 80ng/ml VEGF. Two days later, the medium was switched to StemPro-34 containing 50ng/ml SCF, 50ng/ml IL-3, 5ng/ml TPO, 50ng/ml M-CSF and 50ng/ml Flt3 ligand. On day 10, the supernatant fraction of the cultures was pelleted, resuspended in fresh medium (same as before) and returned to their dishes. On day 14, floating cells were pelleted, resuspended in StemPro-34 containing 50ng/ml M-CSF, 50ng/ml Flt3 ligand and 25ng/ml GM-CSF and replated back to their dishes. The procedure was repeated every four days. From day 24 – 52, a small amount of floating cells was processed for flow cytometry analysis to determine the peak of the CD14/CX3CR1 double positive progenitors. After the isolation of $CD14^+$ or $CD14^+CX3CR1^+$ progenitors, cells were plated onto tissue culture-treated dishes or Thermanox plastic coverslips (all from Thermo Scientific) in a 40-

$50x10^3$ cells/cm^2 in SF–Microglial Medium (RPMI-1640 from Life Technologies supplemented with 2mM GlutaMAX-I, 10ng/ml GM-CSF and 100ng/ml IL-34). Medium was replenished every 3 to 4 days for at least 2 weeks.

Peripheral blood derived macrophages and polarization

Macrophages were differentiated from isolated human mononuclear cells obtained from peripheral blood of healthy individuals at the New York Blood Center as previously described (Pallotta et al., 2015). Briefly, $CD14^+$ cells were isolated after Ficoll gradient and magnetic beads based separation using the EasySep Human CD14 Positive Selection Kit (STEMCELL Technologies). Cells were then seeded in ultra-low attachment plates for 5 days in a $5x10^5$ cells/ml density and differentiated to macrophages using RPMI-1640 supplemented with 2mM GlutaMAX-I, 10% heat-inactivated human serum (Sigma-Aldrich) and 20ng/ml M-CSF (PeproTech). For polarization, macrophages were kept in the same medium (M(-)), or treated for 48 hours with 100ng/ml LPS (Sigma-Aldrich) and 100ng/ml IFNγ (M(LPS, IFNγ)), 40ng/ml IL-4 and 20ng/ml IL-13 (M(IL4,IL13)) or 40ng/ml IL-10 (M(IL10); all from PeproTech).

Immunofluorescent staining

Cells were washed 3X in PBS-T (PBS containing 0.1% Triton-X100) for 10 min, incubated for 2 hours in blocking serum (PBS-T with 5% donkey serum) and primary antibodies (see Antibody Table) were applied overnight at 4°C. The next day, cells were washed 3X in PBS-T for 15 min, incubated with secondary antibodies for 2 hours at room-temperature (RT), washed 3X for 10 min in PBS-T, counterstained with DAPI for 15 min at RT and washed 2X in PBS. Secondary antibodies were used at 1:500 dilution. Images were acquired using an Olympus IX71 inverted microscope, equipped with Olympus DP30BW black and white digital camera. Fluorescent colors were digitally applied using the Olympus software DP Manager or imageJ.

Flow cytometry analysis

Cells were enzymatically harvested by Accutase treatment for 5 min at 37°C and then scrapped with a cell lifter (Sigma-Aldrich). Cells were then re-suspended in 100µl of their respective medium containing the appropriate amount of fluorescence-conjugated antibodies (see Antibody Table) and were incubated on ice for 40 min shielded from light. Isotype controls or secondary antibodies only were used to measure the baseline background signal. DAPI or Sytox Green (Thermofisher) were used for dead cell exclusion. Analyses were performed on a five-laser BD Biosciences ARIA-IIu™ Cell Sorter or on a four-laser Attune NxT Flow Cytometer (ThermoFisher). Data were analyzed using BD FACSDiva™ software or FlowJo version 9.9.4 (FlowJo LLC).

Antibody Table. List of Antibodies used for flow cytometry and immunofluorescent analyses

Name	Host	Vendor	Cat. No.
IBA1	Rabbit	Wako	019-19741
P2RY12	Rabbit	Alomone Labs	APR-020
CD11b-Alexa700	Mouse	BD Pharmingen	557918
CD11c-PE	Mouse	BD Pharmingen	555392
CX3CR1-PE	Mouse	R&D Systems	FAB5204P
CD14-APC	Mouse	BioRad	MCA596APCT
CD45-v450	Mouse	BD Horizon	560367
CD309-APC	Mouse	Miltenyi Biotec	130-093-601
CD235a-PE	Mouse	BD Pharmingen	555570
anti-rabbit IgG-Alexa488	Donkey	ThermoFisher Scientific	A-21206
anti-mouse IgG-Alexa555	Donkey	ThermoFisher Scientific	A-31570

Phagocytosis assay

Phagocytosis assay was performed as previously described (Enomoto et al., 2013). Briefly, Fluoresbrite YG Carboxylate Microspheres 1.00µm (Polysciences) were added to the dishes containing adherent microglial cells in a 200 microspheres/cell ratio. After incubating the cultures at 37^{o}C for 3 hours, fluorescent images were acquired with an Olympus IX71 inverted microscope, equipped with Olympus DP30BW black and white digital camera. Then cells were washed 3X with PBS, treated with Accutase for 5 min and completely detached using a cell lifter. After centrifuging, cells were resuspended in FACS buffer containing DAPI and analyzed on a BD Biosciences ARIA-IIu™ Cell Sorter.

Cytokine Profiler and clustering

For analysis of the secreted cytokine profile of microglial cells, the Human XL Cytokine Array Kit of the Proteome Profiler Antibody Arrays (R&D Systems) was used according to the manufacturer's instructions. Supernatant was collected from the cultures and stored at -80^{o}C for up to 3 months. Membranes were directly visualized in a Kodak Image Station 4000MM PRO and images were acquired using the Carestream Molecular Imaging Software.

For analysis of the signals, images were imported to Image J and the Protein Array Analyzer plugin was used. The intensity reading of the two identical spots was then averaged and the mean value of 8 negative controls was subtracted from every value. Finally, data were expressed as intensity ratio compared to the mean intensity of the 6 reference spots (positive controls). Heatmap and clustering for the protein profiler analysis was generated using heatmap.2 in R version 3.3.1.

Intracellular Ca^{2+} imaging

Cells were cultured onto Thermanox plastic coverslips (ThermoFisher) and were incubated for 30min at 37°C with medium supplemented with the fluorescent Ca^{2+} dye Fluo-4/AM (2mM) mixed at 1:1 with Pluronic-127 reagent (both from Invitrogen). Cells were subsequently washed twice with RPMI-1640 media containing 1% BSA (Life Technologies), 1X GlutaMAX-I and 10mM HEPES (Sigma-Aldrich) pH adjusted to 7.5. Cells were allowed to recover for an additional 30 min to ensure dye esterification. Coverslips were then transferred to a recording chamber mounted onto an upright Olympus BX61 microscope. Fluorescence was recorded at 2Hz by a cooled CCD camera (Hamamatsu Orca R^2). Drug application was done via whole chamber perfusion at room temperature for a period of 60s. $[Ca^{2+}]_i$ transients are expressed in the form of $\Delta F(t)/F_0$, where F_0 is a baseline fluorescence of a given region of interest and ΔF is the difference between current level of fluorescence F(t) and F_0. Fluctuations of $\Delta F(t)/F_0$ that were less than 0.05 were considered as non-responses.

RNA sequencing and analyses

RNA isolation was performed using the RNeasy Plus Mini Kit (Qiagen) with QIAshredder (Qiagen). Cells were enzymatically detached after treatment with Accutase for 5 min and using a cell lifter. After centrifuging, cells were washed with PBS and resuspended in lysis buffer. Samples were then stored at -80^{o}C until processed further according to manufacturer's instructions. RNA was eluted in 30µl RNase free ddH2O and quantified with a NanoDrop 8000 spectrophotometer (Thermo Scientific).

Single-ended RNAseq data were generated with the Illumina HiSeq 2500 platform following the Illumina protocol. The raw sequencing reads were aligned to human hg19 genome using star aligner (version 2.5.0b). Following read alignment, featureCounts (Liao et al., 2014) was used to quantify the gene expression at the gene level based on Ensembl gene model GRCh37.70. Genes with at least 1 count per million (CPM) in at least one sample were considered expressed and hence retained for further analysis, otherwise removed. The gene level read counts data were normalized using trimmed mean of M-values normalization (TMM) method (Robinson et al., 2010) to adjust for sequencing library size difference. Hierarchical cluster analysis based on transcriptome-wide gene expression was performed using R programming language. The RNA sequencing data have been deposited in NCBI's Gene Expression Omnibus and are accessible through GEO Series accession number GSE97744.

For re-analysis of microglia RNAseq data from Zhang et al. (Zhang et al., 2016), we downloaded the raw RNAseq data of "myeloid" cells from gene expression omnibus (GEO: accession GSE73721). The RNAseq read data was processed using the same star/featureCounts pipeline as described above and then the gene level read counts were combined with the gene count data of our samples. The merged data were normalized with the TMM approach and then corrected for batch using linear regression. Hierarchical cluster analysis was used to illustrate the sample dissimilarity.

Similarly, for comparison with a recently published human iPSC-derived microglial dataset from Muffat et al., 2016, we downloaded their RNAseq read data from GEO (accession GSE85839) and then applied the same RNAseq analysis pipeline to obtain gene level count data which was merged with the read count of the present samples. The merged data was normalized and batch corrected before carrying out hierarchical cluster analysis.

Statistics

Frequencies were calculated in excel and expressed as Mean ± Standard Error of the Mean (SEM).

Statistical analysis of $[Ca^{2+}]_i$ transients amplitude was performed using unpaired Student's t-test to compare mean values in excel.

The P value significance of the cluster partition for the dendrogram based on the six signature genes was estimated as the fraction of 1000 repeated permutations (shuffling gene expression values within each gene) in which the cluster center distance obtained from k-means cluster with two centers was more extreme than that in the original data.

Pearson's correlation coefficient between iPSC-MG and hMG or hMG-SF for cytokine release data was calculated using GraphPad Prism 6.

Supplemental References

Douvaras, P., Wang, J., Zimmer, M., Hanchuk, S., O'Bara, M.A., Sadiq, S., Sim, F.J., Goldman, J., and Fossati, V. (2014). Efficient generation of myelinating oligodendrocytes from primary progressive multiple sclerosis patients by induced pluripotent stem cells. Stem cell reports *3*, 250-259.

Enomoto, R., Imamori, M., Seon, A., Yoshida, K., Furue, A., Tsuruda, H., and Lee-Hiraiwa, E. (2013). Proposal for a new evaluation of phagocytosis using different sizes of fluorescent polystyrene microspheres. Advances in Biological Chemistry *03*, 556-563.

Liao, Y., Smyth, G.K., and Shi, W. (2014). featureCounts: an efficient general purpose program for assigning sequence reads to genomic features. Bioinformatics *30*, 923-930.

Pallotta, I., Sun, B., Wrona, E.A., and Freytes, D.O. (2015). BMP protein-mediated crosstalk between inflammatory cells and human pluripotent stem cell-derived cardiomyocytes. Journal of tissue engineering and regenerative medicine.

Panicker, L.M., Miller, D., Awad, O., Bose, V., Lun, Y., Park, T.S., Zambidis, E.T., Sgambato, J.A., and Feldman, R.A. (2014). Gaucher iPSC-derived macrophages produce elevated levels of inflammatory mediators and serve as a new platform for therapeutic development. Stem cells *32*, 2338-2349.

Paull, D., Sevilla, A., Zhou, H., Hahn, A.K., Kim, H., Napolitano, C., Tsankov, A., Shang, L., Krumholz, K., Jagadeesan, P*., et al.* (2015). Automated, high-throughput derivation, characterization and differentiation of induced pluripotent stem cells. Nature methods *12*, 885-892.

Robinson, M.D., McCarthy, D.J., and Smyth, G.K. (2010). edgeR: a Bioconductor package for differential expression analysis of digital gene expression data. Bioinformatics *26*, 139-140.

Woodard, C.M., Campos, B.A., Kuo, S.H., Nirenberg, M.J., Nestor, M.W., Zimmer, M., Mosharov, E.V., Sulzer, D., Zhou, H., Paull, D*., et al.* (2014). iPSC-derived dopamine neurons reveal differences between monozygotic twins discordant for Parkinson's disease. Cell reports *9*, 1173-1182.